Article

Discovery Medicine 2023; 35(179): 1077–1085
https://doi.org/10.24976/Discov.Med.202335179.104

ASCs-EVs Inhibit Apoptosis and Promote Myocardial Function in the Infarcted Heart via miR-221

Jirong Zhang[1,†], Jimei Zhang[2,*,†], Xicheng Jiang[3,*], Juan Jin[4], He Wang[5], Qiao Zhang[6]

[1]Graduate School, Heilongjiang University of Chinese Medicine, 150040 Harbin, Heilongjiang, China
[2]College of Public Health, The University of Sydney, 2006 Sydney, Australia
[3]College of Basic Medicine, Heilongjiang University of Chinese Medicine, 150040 Harbin, Heilongjiang, China
[4]Department of Cardiovascular Disease, The First Affiliated Clinical Medical College of Heilongjiang University of Chinese Medicine, 150040 Harbin, Heilongjiang, China
[5]Department of Interventional, Harbin Medical University Cancer Hospital, 150081 Harbin, Heilongjiang, China
[6]School of Pharmacy, Harbin University of Commerce, 150076 Harbin, Heilongjiang, China
*Correspondence: iriszjm@163.com (Jimei Zhang); jiangxicheng5303@163.com (Xicheng Jiang)
†These authors contributed equally.
Published: 1 December 2023

Background: Extracellular vehicles (EVs) secreted from adipose-derived stem cells (ASCs) (ASCs-EVs) have the potential to treat myocardial infarction (MI), although the underlying mechanism remains unclear. The current study explored the ability of ASCs-EVs to inhibit apoptosis and promote myocardial function in the infarcted heart via microRNAs (miRNAs)-221.
Methods: In hypoxia-induced H9C2 cells, a cardiac cell strain derived from the SD Rat left ventricle, we measured the cell viability and apoptosis-related protein expression after transfection with the ASCs-EVs-NC (negative control for EVs-miR-221) or ASCs-EVs-miR-221 mimics. We then verified the cardioprotective effects of miR-221-overexpressing ASCs-EVs by investigating myocardial cell apoptosis and cardiac function in a MI rat model treated with ASCs-EVs from miR-221-overexpressing ASCs by comparing control with ASC treatment.
Results: The *in vitro* experiment results showed that the proliferation of H9C2 cells and the anti-apoptotic protein expression were significantly enhanced by the ASCs-EVs-miR-221 mimic. The *in vivo* experiment results found that ASCs-EVs from miR-221-overexpressing ASCs have cardioprotective effects, as demonstrated by lower serum troponin levels and left ventricular end-systolic volume, and a lower number of apoptotic myocardial cells than those in control and ASC-treated rats.
Conclusions: ASCs-EVs have therapeutic effects on MI by inhibiting cardiomyocyte apoptosis via miR-221.

Keywords: myocardial infarction; adipose-derived stem cells; extracellular vesicles; miR-221; anti-apoptosis

Introduction

Impaired cardiac function due to myocardial infarction (MI) ranks among the most common reasons for death around the world [1–3]. Although comprehensive clinical treatment for MI, including early revascularization, is effective in reducing mortality [4–6], acute and chronic myocardial cell loss is irreversible, leading to heart dysfunction. Difficulties associated with myocardial regeneration underscore the need to design new therapeutic strategies for MI treatment. Cell therapies based on stem cell can offer potentially innovative and possible solutions in cases in which it is necessary to repair or regenerate damaged tissues by trauma or degenerative processes. [7]. Stem cell therapy aiming at cardiomyocyte regeneration has attracted increasing attention [8,9]. Studies show that stem cell transplantation treatment improves the cardiac function of animals with MI as well as in patients with MI [10]. However, clinical trials show that bone marrow mesenchymal stem cells (MSCs), adipose-derived stem cells (ASCs), and other stem cells are difficult to differentiate into new functional cardiomyocytes *in vivo*.

Therefore, an increasing number of researchers have investigated extracellular vehicles (EVs). EVs are small vesicles which constitutively released from multiple tissues and cell types [11,12]. EVs can serve as an excellent intercellular communication tool, transferring bioactive molecules such as microRNAs (miRNAs), mRNAs, DNA, proteins and lipids [13,14]. EVs play crucial roles in immunoregulation and the regeneration of articular cartilage [15,16]. In addition, EVs secreted by stem cells promote cardiac function [17,18]. However, the mechanism underlying the influence of EVs on cardiac function after MI remains unclear.

miRNAs are small non-coding RNAs, which can regulate post-transcriptional gene expression and are associated with human diseases including MI [19–21]. miRNAs not only play an important role in the prognosis and pathogen-

esis of cardiovascular diseases but also can be a therapeutic target [22,23]. miRNAs in EVs have received increasing attention, providing a potential new therapeutic strategy for various diseases. miR-221-5p is involved in the regulation of osteogenic differentiation of MSCs in myeloma bone disease [24]. miR-221 overexpression promotes MSC migration [25]. miR-221 is expressed at high levels in MI, indicating that miR-221 may be related to myocardial injury, and miR-221 has anti-apoptotic effects in many cells and animal models [26]. We hypothesized that ASCs-derived EVs (ASCs-EVs) overexpressing miR-221 may provide a novel therapeutic strategy in MI. The anti-apoptotic effects of ASCs-EVs overexpressing miR-221 were examined in H9C2 cells. The effect of miR-221-overexpressing ASCs-EVs on myocardial function was examined in post-MI rats by assessing cardiomyocyte apoptosis. The results indicated that the cardioprotective effect of miR-221-enriched ASCs-EV is greater than that of ASCs in post-MI rats.

Materials and Methods

Isolation and Identification of ASCs

specific pathogen-free (SPF)-grade male SD rats (8 weeks old, body weight 220–240 g) were purchased from Shanghai Slack Laboratory Animal Co., LTD., certificate No. SCXK (Filter) 2020-0007. The rats were kept in SPF animal houses with an ambient temperature of 20 °C–24 °C, ambient humidity of 50%–70%, and a normal daylight cycle. Two or three animals were housed in a cage, with no restrictions on food and water. Adipose tissue was obtained from subcutaneous fatty tissues of rats. The intraperitoneal injection was administered with 3% sodium pentobarbital. Subcutaneous fat was collected, put into a 2-mL frozen-storage tube, quickly placed in liquid nitrogen, and then transferred to –80 °C for storage before measurements. Adipose tissue was digested at 37 °C for 30 min using 0.01% type I collagenase (#SCR103, Sigma-Aldrich, St. Louis, MO, USA). After digestion, the mixture was filtered by the cell strainer and then centrifuged at 1000 rmp for 5 min. Cells were then seeded at a dose of 5×10^3 cells/cm^2 in Dulbecco's modified eagle medium (DMEM) (#11965092, Gibco, Carlsbad, CA, USA) supplemented with 10% fetal bovine serum (FBS) (#16140071, Gibco, Carlsbad, CA, USA), L-glutamine (#21051024, Thermo Fisher Scientific, Rockford, IL, USA), and streptomycin (#15070063, Thermo Fisher Scientific, Rockford, IL, USA). Cells were cultured at 37 °C for 2 days, and the cells that were tightly adhered to the bottom of the culture flasks were ASCs. ASCs were co-cultured with 10 ng/mL interferon gamma (#11276905001, Sigma-Aldrich, St. Louis, MO, USA) for 48 h for EV isolation.

ASCs were identified through flow cytometry analysis. ASCs were harvested through trypsinization and washed three times with phosphate-buffered saline (PBS) (#P2272, Sigma-Aldrich, St. Louis, MO, USA). ASCs were then incubated with antibodies against CD34, CD45, CD73, CD90 and CD105, and then subjected to flow cytometry. The analysis was performed using FlowJO software (V10. TreeStar, Inc. Ashland, OR, USA).

Isolation and Identification of ASCs-EVs

To isolate ASCs-EVs, ASCs were washed three times with PBS, then cultured with DMEM without FBS for 48 h. The supernatant was collected, and large fragments and dead cells were removed using a 0.22-micron filter. Debris was removed through centrifugation at 3700 rmp for 15 min. The resultant supernatant was centrifuged at 1000 rmp for an additional 15 min, followed by 2000 rmp for 15 min, and finally twice at 4000 rmp for 15 min. The above centrifugation steps were conducted at 4 °C. EVs were pelleted by ultracentrifugation at 100,000 rmp for 9 h at 4 °C by a 70Ti rotor (#337922, Beckman, Bria, CA, USA), then identified by measuring the expressions of CD9, CD63, and HSP70 using the western blot (WB) assay. The specific protocol is described in the "WB assay".

Cell Culture

H9C2 cells were provided by the Chinese Academy of Sciences. Cells were cultured in DMEM supplemented with 10% FBS and streptomycin at 37 °C. No mycoplasma contamination was detected through the mycoplasma testing.

Cell Groups and Cell Transfection (H9C2 Cells)

Cells were divided into 5 groups: control, model, ASC, EVs-NC (negative control for EVs-miR-221), and EVs-miR-221. All groups except for the control group were hypoxia-treated. For the hypoxic cell model, a hypoxic culture environment (0.2% oxygen) was used to induce cell damage. Before hypoxia treatment, H9C2 cells in the ASC group were incubated with ASC medium, while the EVs-NC and EVs-miR-221 groups were treated with NC or miR-221 mimics transfected with EVs. The miR-221 or NC mimics were incubated with Lipofectamine 2000 (#11668019, Thermo Fisher Scientific, Waltham, MA, USA), and then added into ASC cells for 24 h. Next, the EVs were collected using the previously described method in the "isolation of EVs" section. Total RNA was collected for analysis of potential miR-221 target genes. The miR-221 forward primer sequence was as follows: 5′-TTTCCaggTAGCCtGaaACC-3′, reverse primer sequence: 5′-GGCATGAACCTGGCATACAA-3′. GAPDH forward primer sequence: 5′-ACACGACGGCTTCGCTC-3′, reverse primer sequence: 5′-TGCGTTTAAGCACTTCGCA-3′.

Cell Viability Assay

ASCs were seeded into the 96-well plate at 3000 cells/cm^2 and incubated for 6 days. H9C2 cells were seeded into the 96-well plate at 5000 cells/cm^2 and incubated under

hypoxia or normoxia. The 3-(4,5-dimethylthiazol-2-yl)-2,5-diphenyltetrazolium bromide (MTT) assay was used to examine cell viability. In general, cells were cultured for 24 h before the addition of MTT (#V13154, Thermo Fisher Scientific, Waltham, MA, USA) solution to generate formazan, which only reacts with live cells. Dimethyl sulfoxide (DMSO) (#D12345, Thermo Fisher Scientific, Waltham, MA, USA) was added to solubilize the formazan, and the absorbance of the cells in wells was recorded at 570 nm through the microplate reader (#800 TS, BioTek, Winooski, VT, USA).

RNA Isolation and Quantitative Real-Time PCR (qRT-PCR)

Total RNAs were extracted through the Trizol reagent (#9108, Takara, Tokyo, Japan) based on the manufacturer's protocol. The quality and concentration of RNA were measured through spectrophotometry. One microgram of RNA was used to perform qRT-PCR according to the manufacturer's protocol (Takara). Each qRT-PCR run was performed in triplicate. mRNA expression was normalized to that of β-tubulin.

Terminal Deoxynucleotidyl Transferase dUTP Nick-End Labeling (TUNEL) Staining

Apoptosis was detected using the TUNEL assay kit (#C1089, Beyotime, Shanghai, China) according to the manufacturers' directions. Firstly, cells were seeded into the 6-well plate and adhered to it. Next, cells were fixed with 4% paraformaldehyde for 15 min, then washed three times with PBS, and incubated with 10% Triton for 10 min. After washing, the cells were incubated with TUNEL reaction liquid at 37 °C for 1 h followed by DAPI. Cells were visualized by fluorescence microscopy (#BX51, OLYMPUS Corporation, Tokyo, Japan). Nine randomly selected fields were used for the detection of TUNEL-positive cells (with red fluorescent nuclei). For TUNEL immunohistochemical staining, heart slides were incubated with Convert agent Peroxidase (POD) for 30 min. DAB solution was used for the color reaction.

Animal Groups and the Animal Model

SD rats were divided into the following groups: control, model, ASC, EVs-NC, and EVs-miR-221, with 6 SD rats in each group. Permanent ligation of the left anterior descending coronary artery (LAD) was performed to generate an acute MI model in SD rats (200–250 g). Anesthesia was induced using 5% isoflurane inhalation and maintained using 2% isoflurane. Permanent ligation was performed using a 6-0 Ethicon silk suture around the LAD coronary artery 2–3 mm from its origin. Successful MI models were confirmed based on local wall motion abnormality and pallor of the infracted left ventricle. ASCs-EVs were intramuscularly injected into rats (the EVs were collected using the method described above in the "isolation of EVs" section) at 30 min after MI surgery. SD rats were euthanized by excessive isoflurane inhalation (40%) 2 weeks after MI. Myocardial tissues and serum were collected for subsequent experiments.

Cardiac Function Examination

Four weeks after injection, echocardiography was performed to measure cardiac function. The following parameters were acquired through M-mode tracing: left ventricular end-diastolic volume (LVEDD) and left ventricular end-systolic volume (LVESD), measured for at least 5 consecutive cardiac cycles. The formula for calculating left ventricular ejection fraction (LVEF) was: LVEF = [(LVEDD3 – LVESD3) / LVEDD3] $\times$ 100%, and the result was expressed as a percentage.

Tetrazolium Chloride Staining

Myocardial tissues were first fixed with 4% formaldehyde for 48 h, then dehydrated in an alcohol gradient, embedded in paraffin, and cut into 5-µm thick sections. For triphenyl tetrazolium chloride (TTC) staining, heart slides were incubated with 1% 2, 3, 5-triphenyl tetrazolium chloride (#T8877; Sigma-Aldrich, St. Louis, MO, USA) at 37 °C for 30 min. The areas displaying normal and infarcted myocardium were evaluated by planimetry using dedicated software (ImageJ software, Version 1.53c, National Institutes of Health, Boston, MA, USA). MI was quantified using the following equation:

Infarcted myocardium area / (infarcted myocardium area + normal myocardium area) $\times$ 100%.

Enzyme-Linked Immunosorbent (ELISA) Assay

Blood samples were collected and isolated to detect troponin levels using ELISA kits (#PA002, Beyotime Institute of Biotechnology, Shanghai, China) in accordance with the manufacturer's protocol.

Western Blotting Assay

The extracted protein was separated by 6% or 10% sodium dodecyl sulfate-polyacrylamide gel electrophoresis, then transferred to polyvinylidene difluoride membranes (#R006485, BD Biosciences, San Jose, CA, USA). Next, the membranes were incubated with antibodies against CD9, CD63, HSP70, Bcl-2, Bax, cleaved caspase3, and GAPDH (1:1000; Proteintech) overnight at 4 °C. Membranes were washed with PBS 3 times, then incubated with horseradish peroxidase-labeled secondary antibody (1:5000) (#SA00013-4, Proteintech, Chicago, IL, USA) at room temperature for 1 h. Protein expression was standardized to that of β-tubulin. Blots were examined by chemiluminescence through the ChemiDoc XRS Imaging System (#1708265, Bio-Rad, Heracles, CA, USA). The strip gray value was analyzed using ImageJ software and the data were analyzed using Quantity one software (V4.6.6, Bio-Rad, Heracles, CA, USA).

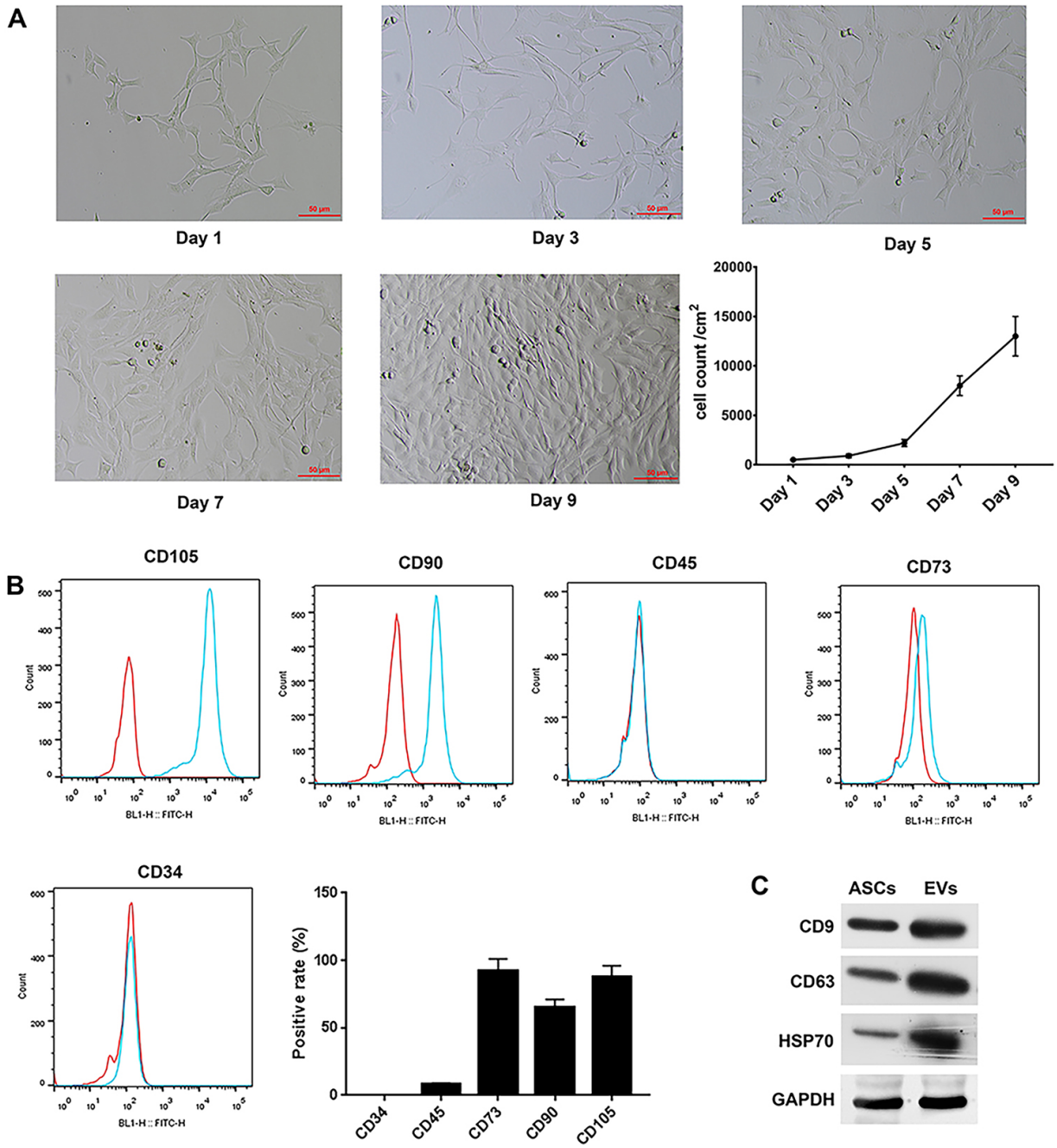

Fig. 1. Identification of adipose-derived stem cells (ASCs) and ASCs-derived extracellular vehicles (ASCs-EVs). (A) The morphology of ASCs. The scale bar represents 50 µm. The population doubling level refers to the total number of times the cells in the population have doubled since *in vitro* primary isolation. (B) Identification of ASCs using the flow cytometry assay. (C) Western blot assay and quantification of the expression of CD63, CD9, and HSP70 in ASCs and ASCs-derived EVs.

Statistical Analysis

Statistical analysis was conducted using GraphPad Prism 7 software (GraphPad Software, San Diego, CA, USA) and SPSS software (version 22.0, IBM Corp., Armonk, NY, USA). Unless otherwise specified, data are presented as the mean ± standard error of the mean (SEM). The Student two-tailed *t*-test and one-way analysis of variance with Tukey's post hoc test were performed. *p*-values < 0.05 were considered statistically significant.

Results

Isolation and Identification of ASCs and ASCs-Derived EVs

At 3 days after inoculation, ASCs showed a shuttle-like and polygonal shape. At 5 days after inoculation, ASCs showed long streaks and grew fast. The analysis verified the high expressions of CD90, CD73, and CD105. Furthermore, the cell growth rate and cell number were exam-

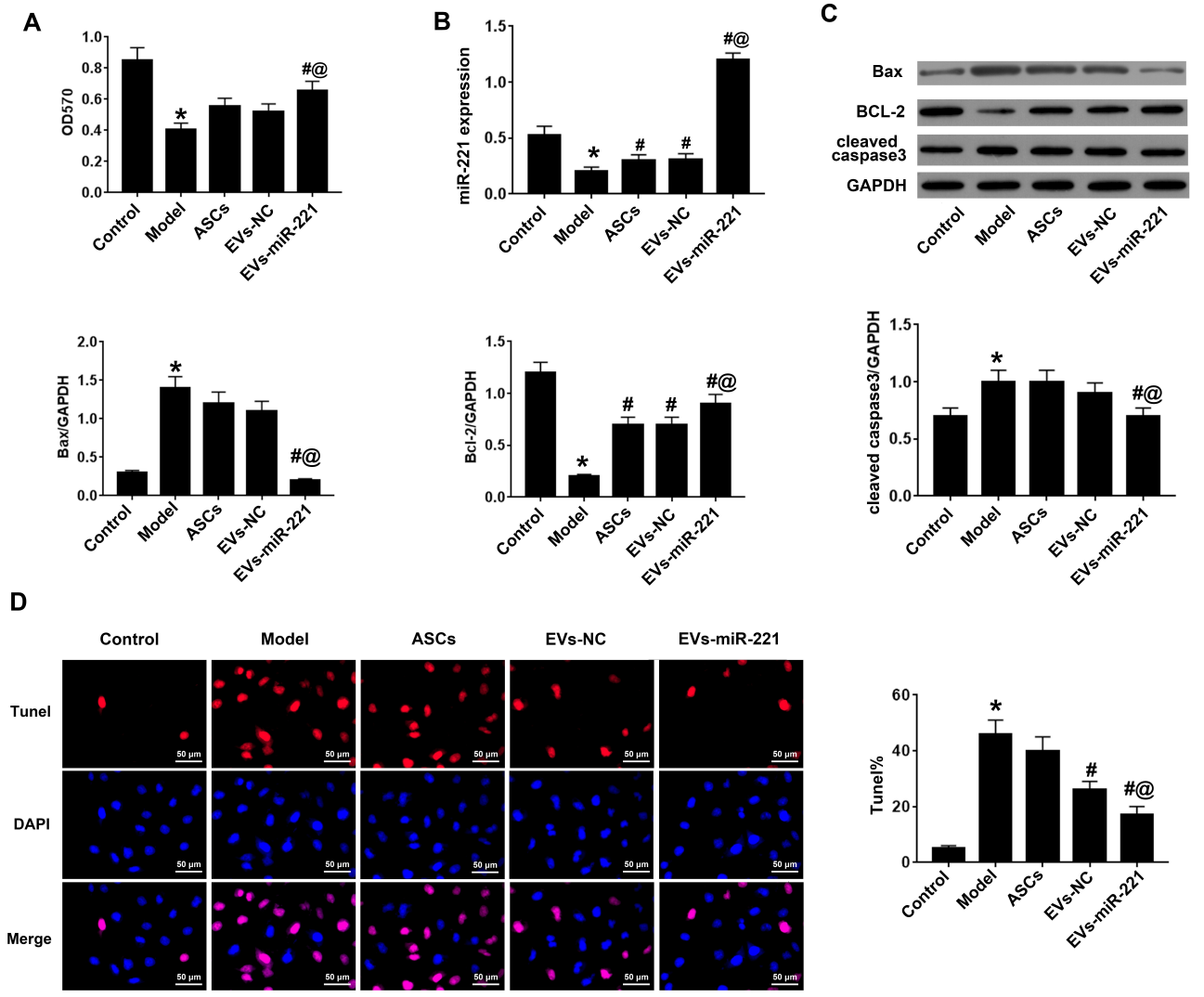

Fig. 2. MicroRNAs (miRNAs)-221-overexpressing ASCs-derived EVs inhibited cardiomyocyte apoptosis. (A) Cell proliferation was evaluated using the 3-(4,5-dimethylthiazol-2-yl)-2,5-diphenyltetrazolium bromide (MTT) test. (B) The miR-221 expression level was measured using PCR. (C) The expressions of cleaved caspase3, and Bcl2/Bax in H9C2 cells were measured using the western blot assay for the four groups. (D) TUNEL staining and cartogram of H9C2 cells in four groups. * $p < 0.05$ vs. control group. # $p < 0.05$ vs. model group. @ $p < 0.05$ vs. ASC medium group (n = 6).

ined by calculating the population doubling level (PDL). The PDL level and cell density increased on day 5, consistent with the results of the cell proliferation assay (Fig. 1A). We then used a flow assay to identify the ASCs (Fig. 1B). The flow assay showed high levels of CD73, CD90, and CD105, and lower levels of CD34 and CD45. These results indicated the successful isolation of ASCs.

Through differential ultracentrifugation, as mentioned in the methods section, EVs were isolated from the cell culture medium. ASCs-EVs were identified by assessing protein marker expression. Western blotting results showed that the isolated EVs had high expression levels of CD63, CD9, and HSP70 compared with ASCs (Fig. 1C), which are markers of ACS-EVs. The results indicated the successful isolation of ASCs-EVs.

miR-221-Overexpressing ASCs-EVs Inhibited Cardiomyocyte Apoptosis

The effects of miR-221-overexpressing ASCs-EVs on cardiomyocytes were investigated by generating a hypoxia-induced cell damage model. In order to explore the influence of miR-221-overexpressing ASCs-EVs, cells were divided into five groups as follows: control, model, ASCs, EVs-NC, and EVs-miR-221. After hypoxia injury, cell proliferation was reduced, which was rescued by EVs-miR-221 treatment (Fig. 2A). EVs-miR-221 treatment significantly upregulated miR-221 ($p < 0.05$) compared to the sole ASC treatment (Fig. 2B). Furthermore, H9C2 cells grown under hypoxic conditions displayed high expression levels of cleaved caspase3 and Bax, and low Bcl-2 levels,

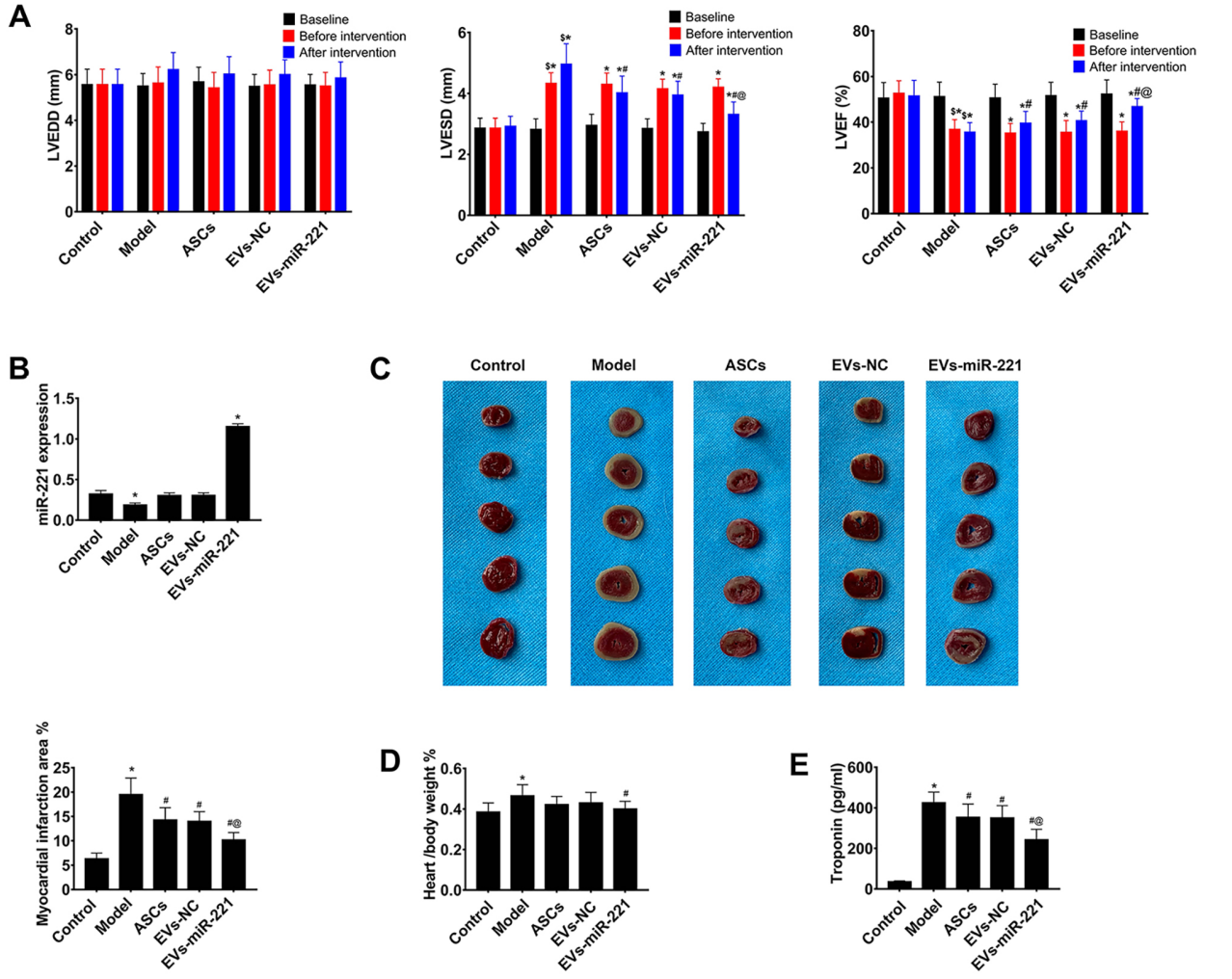

Fig. 3. ASCs-derived EVs overexpressing miR-221 improved cardiac function in post-myocardial infarction (MI) rats. (A) Cardiac function analysis of rats in each group. * $p < 0.05$, compared to baseline; $ $p < 0.05$, compared to the control; # $p < 0.05$, compared to the model; @ $p < 0.05$, compared to the ASCs. (B) miR-221 expression in rats of each group. (C) MI area cartogram of each group. Normal myocardial tissue was defined as brick red staining by triphenyl tetrazolium chloride (TTC) staining, and infarcted myocardial tissue was defined as pale staining by TTC staining. (D) The ratio of heart weight to body weight in each group. (E) Troponin level in each group. * $p < 0.05$ vs. control group. # $p < 0.05$ vs. model group. @ $p < 0.05$ vs. ASC medium group (n = 6).

whereas incubation with EVs-miR-221 decreased caspase3 and Bax expressions by nearly five-sixths ($p < 0.05$) but significantly elevated the expression of Bcl-2 ($p < 0.05$; Fig. 2C). TUNEL staining was performed to measure apoptotic cell death. As shown in Fig. 2D, EVs-miR-221 treatment decreased TUNEL fluorescence compared to ASC treatment ($p < 0.05$) and significantly decreased TUNEL fluorescence compared to that of the EVs-NC group ($p < 0.05$). These results indicated that ASCs-EVs overexpressing miR-221 decreased cardiomyocyte apoptosis.

miR-221-Overexpressing ASCs-EVs Improved Cardiac Function in Post-MI Rats

The effect of miR-221-overexpressing ASCs-EVs on myocardial function was examined in a MI rat model. At 28 days post-MI, cardiac function was significantly reduced as evidenced by increased LVESD and decreased LVEF levels ($p < 0.05$), which were partially reversed by treatment with EVs-miR-221 (Fig. 3A). ASC and EVs-NC treatments had a smaller protective effect on MI rats, inducing a slight reduction in LVESD ($p < 0.05$) but a small increase in LVEF ($p < 0.05$). ASCs-EVs-miR-221 mimic treatment significantly reduced LVED ($p < 0.05$) and increased LVEF ($p < 0.05$) compared to ASC treatment. No significant differences were found in LVEDD between the control, model, ASC, EVs-NC mimic, and EVs-miR-221 mimic groups. The miR-221 expression level markedly increased in the EVs-miR-221 group ($p < 0.05$; Fig. 3B). The above results showed that miR-221-overexpressing ASCs-EVs attenuated MI-induced cardiac damage via a miR-221-dependent mechanism.

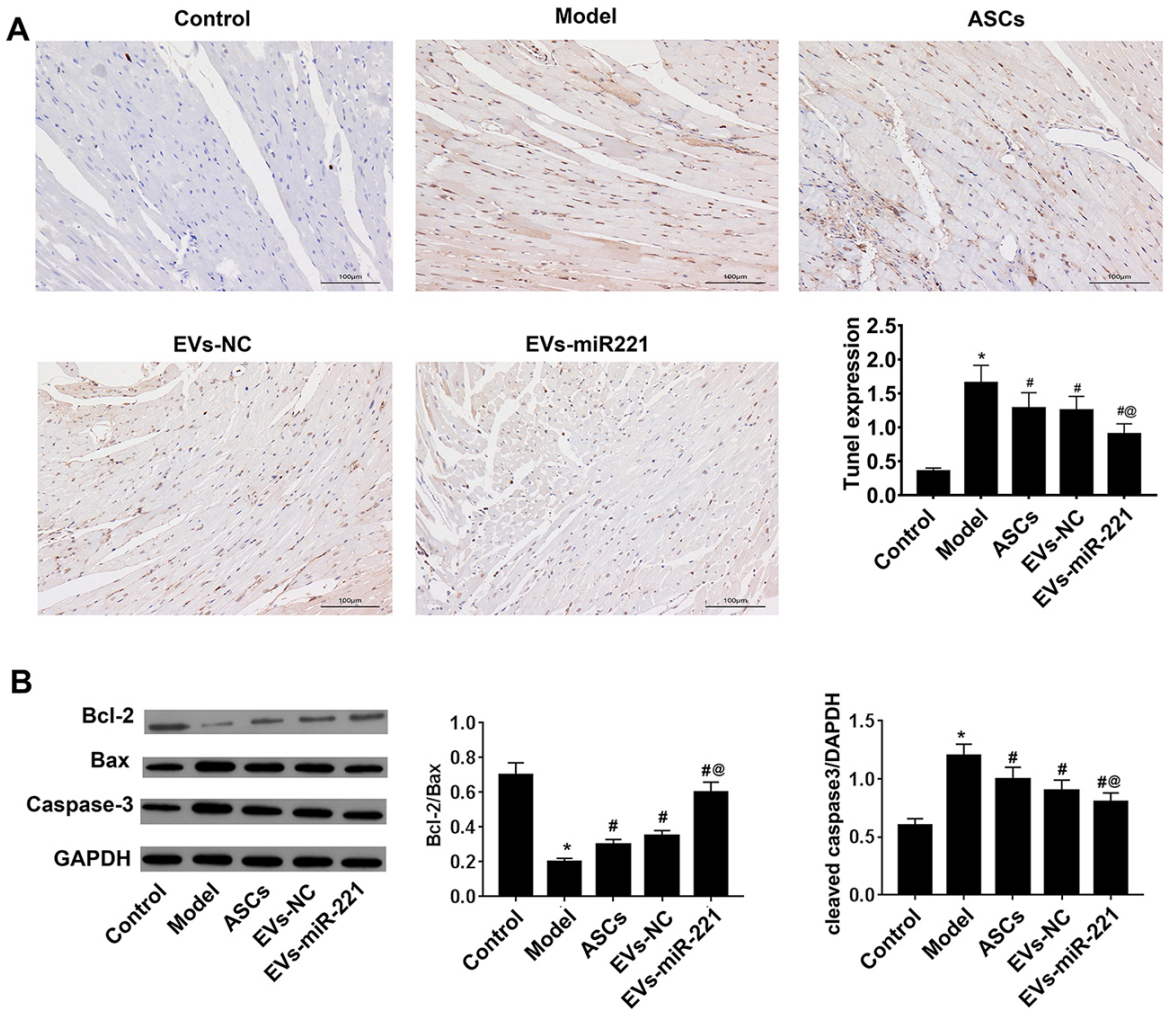

Fig. 4. ASCs-derived EVs overexpressing miR-221 attenuated myocardial cell apoptosis in post-MI rats. (A) TUNEL immunohistochemical staining and statistical analysis in each group. The scale bar represents 100 µm. (B) Western blot analysis and quantification of Bcl2, Bax, and cleaved caspase3 expression *in vivo*. * $p < 0.05$ vs. control group. # $p < 0.05$ vs. model group. @ $p < 0.05$ vs. ASC medium group (n = 6).

Compared with the control group, assessment of the extent of MI by TTC staining showed that the MI groups had a larger MI region ($p < 0.05$; Fig. 3C). However, the EVs-miR-221 group showed a markedly smaller MI area than that in the model group ($p < 0.05$) or ASC group ($p < 0.05$). The heart weight to body weight ratio and serum troponin levels were measured to evaluate the extent of cardiac injury. A high heart-weight-to-body weight ratio ($p < 0.05$) and serum troponin ($p < 0.05$) were observed in the model group (Fig. 3D,E), whereas EVs-miR-221 treatment restored heart weight to body weight ratio to almost normal levels ($p < 0.05$) and decreased serum troponin by 50% ($p < 0.05$) compared to ASC treatment. In conclusion, ASCs-EVs have a protective effect on cardiac function via miR-221 overexpression in post-MI rats.

miR-221-Overexpressing ASCs-EVs Decreased Myocardial Cell Apoptosis in Post-MI Rats

To investigate the mechanism underlying the protective effect of miR-221-overexpressing ASCs-EVs, we performed TUNEL immunohistochemical staining to evaluate apoptosis of myocardial cells in post-MI rats (Fig. 4A). The TUNEL-positive area, indicated myocardial apoptosis, was significantly larger in the MI group compared with the control group ($p < 0.05$) and observably smaller in the EVs-miR-221 group compared with the model group and ASC group ($p < 0.05$, both).

Assessment of the expression of apoptosis-related proteins in each group (Fig. 4B) showed lower Bcl2/Bax expression in the model group than the control group ($p < 0.05$), while the ASC group and EVs-NC group both showed a small increase over the model group ($p < 0.05$). The EVs-miR-21 group exhibited an almost 5-fold increase compared to the model group ($p < 0.05$) and a 2-fold in-

crease compared to the ASC group ($p < 0.05$). Compared with the control group, the expression of cleaved caspase3 was significantly higher in the model, ASC, and EVs-NC groups ($p < 0.05$). EVs-miR-21 mimic treatment markedly downregulated cleaved caspase3 expression ($p < 0.05$). These results showed that miR-221-overexpressing ASCs-EVs attenuated myocardial cell apoptosis in post-MI rats, consistent with the *in vitro* results.

Discussion

MI is a severe disease that can lead to myocardial necrosis [27]. Although several treatments improve the prognosis of MI patients, the regeneration of myocardial cells is difficult, and myocardial apoptosis is accelerated during MI [28]. The apoptotic process is regulated by a variety of apoptosis-related genes, particularly Bcl2, Bax, and caspase3 [29]. Inhibiting myocardial cell apoptosis, protecting myocardial cell function, and reducing the area of myocardial damage have been research hotspots in MI treatment in recent years.

The ability of MSCs to differentiate into functional cardiomyocytes has sparked a research boom into myocardial regeneration methods. However, later research found that the protective effect of MSCs may be attributed to the secretion of EVs [30,31]. EVs are membrane vesicles with a diameter of <200 nm that are secreted by cells. EVs are important mediators of intercellular communication. They enter target cells via membrane receptors or by endocytosis and deliver bioactive molecules including proteins, mRNAs, and microRNAs that are involved in biological information regulation [32,33]. mRNAs and microRNAs have been found in EVs secreted by MSCs (MSCs-EVs); these EVs can be incorporated by adjacent or distant cells to regulate receptor cells, indicating that MSCs-EVs can serve as vectors for miRNA transfer and mediate intercellular communication [34]. The miRNAs in EVs affect gene expression in receptor cells [35]. miR-93-5p-containing EVs secreted from adipose-derived stromal cells show a stronger protective effect on MI injury than simple EVs [36]. The protective effect of EVs from miR-126-overexpressing ADSCs was verified in a MI model [37]. MiR-221 is strongly implicated in MI development and progression. However, no previous studies have explored the effect of miR-221-overexpressing EVs on MI.

In this study, we designed ASCs-EVs with overexpressed miR-221 and investigated their protective properties in H9C2 cells and post-MI rats. The cell injury model was generated by culturing cells in a hypoxic environment for 24 h. The anti-apoptotic effects of ASCs-EVs with overexpressed miR-221 were demonstrated in H9C2 cells, which showed higher Bcl2/Bax levels and lower cleaved caspase3 levels compared with the model group. An *in vivo* MI model was successfully established in rats. LVESD was higher and LVEF was significantly lower in the miR-221-overexpressing ASCs-EV group than in the MI group. Furthermore, the number of apoptotic cells markedly decreased, the Bcl2/Bax ratio increased, and cleaved caspase3 was significantly downregulated in the miR-221-overexpressing ASCs-EV group compared to the model group. Together, the results of the present study indicated that ASCs-EVs overexpressing miR-221 inhibit cardiomyocyte apoptosis and promote cardiac function after MI.

Conclusions

This study demonstrated that ASCs-EVs inhibit myocardial apoptosis and improve myocardial function via miR-221 overexpression. ASCs-EVs with overexpressed miR-221 can be one of the novel therapeutic strategies for MI treatment.

Availability of Data and Materials

The datasets analyzed during the current study are available.

Author Contributions

JRZ and QZ designed the research study. XCJ and JJ performed the research. HW and JMZ analyzed the data. All authors contributed to the drafting and revision of the manuscript, and approved the final manuscript. All authors have participated sufficiently in the work and agreed to be accountable for all aspects of the work.

Ethics Approval and Consent to Participate

All animals were acclimated under standard laboratory conditions and had standard water and food. All protocols used for animal experiments were conducted according to the Principles of Laboratory Animal Care and approved by the Animal Ethical Committee of the Harbin University of Commerce (HSDYXY-20230010).

Acknowledgment

Not applicable.

Funding

This study was funded by National Natural Science Foundation of China (82174261).

Conflict of Interest

The authors declare no conflict of interest.

References

[1] Jenča D, Melenovský V, Stehlik J, Staněk V, Kettner J, Kautzner J, *et al*. Heart failure after myocardial infarction: incidence and predictors. ESC Heart Failure. 2021; 8: 222–237.

[2] Antonio HR. From Assessing Risk Factors to Understanding, Preventing, and Treating Cardiovascular Diseases: An Urgent Journey. Discovery Medicine. 2022; 34: 199–204.

[3] Mechanic OJ, Gavin M, Grossman SA. Acute Myocardial Infarction. StatPearls. Treasure Island (FL) ineligible companies.

Disclosure: Michael Gavin declares no relevant financial relationships with ineligible companies. Disclosure: Shamai Grossman declares no relevant financial relationships with ineligible companies.: StatPearls Publishing Copyright © 2023, StatPearls Publishing LLC. 2023.

[4] Heusch G. Molecular basis of cardioprotection: signal transduction in ischemic pre-, post-, and remote conditioning. Circulation Research. 2015; 116: 674–699.

[5] Şentürk T, Çavun S, Avcı B, Yermezler A, Serdar Z, Savcı V. Effective inhibition of cardiomyocyte apoptosis through the combination of trimetazidine and N-acetylcysteine in a rat model of myocardial ischemia and reperfusion injury. Atherosclerosis. 2014; 237: 760–766.

[6] Fu C, Gao Q, Zhao Z, Yu, Liu J, An Y. The Clinical Characteristics of Acute Myocardial Infarction with Ventricular Septal Perforation and the Prognosis Comparison of Different Treatment Methods. Heart Surgery Forum. 2021; 24: e757–e763.

[7] Tel A, Miotti G, Ius T, Marco L, Robiony M, Parodi PC, *et al*. Stem Cells in Facial Regenerative Surgery: Current Clinical Applications. A Multidisciplinary, Systematic Review. Frontiers in Bioscience-Landmark. 2023; 28: 123.

[8] Cho HM, Cho JY. Cardiomyocyte Death and Genome-Edited Stem Cell Therapy for Ischemic Heart Disease. Stem Cell Reviews and Reports. 2021; 17: 1264–1279.

[9] Bonavida V, Ghassemi K, Ung G, Inouye K, Thankam FG, Agrawal DK. Novel Approaches to Program Cells to Differentiate into Cardiomyocytes in Myocardial Regeneration. Reviews in Cardiovascular Medicine. 2022; 23: 392.

[10] Zhao M, Nakada Y, Wei Y, Bian W, Chu Y, Borovjagin AV, *et al*. Cyclin D2 Overexpression Enhances the Efficacy of Human Induced Pluripotent Stem Cell-Derived Cardiomyocytes for Myocardial Repair in a Swine Model of Myocardial Infarction. Circulation. 2021; 144: 210–228.

[11] Chuo STY, Chien JCY, Lai CPK. Imaging extracellular vesicles: current and emerging methods. Journal of Biomedical Science. 2018; 25: 91.

[12] Ge F, Wang Z, Xi JJ. Engineered Maturation Approaches of Human Pluripotent Stem Cell-Derived Ventricular Cardiomyocytes. Cells. 2019; 9: 9.

[13] Liu S, Wu X, Chandra S, Lyon C, Ning B, Jiang L, *et al*. Extracellular vesicles: Emerging tools as therapeutic agent carriers. Acta Pharmaceutica Sinica. B. 2022; 12: 3822–3842.

[14] Xu YZ, Cheng MG, Wang X, Hu Y. The emerging role of noncoding RNAs from extracellular vesicles in Alzheimer's disease. Journal of Integrative Neuroscience. 2021; 20: 239–245.

[15] Yin B, Ni J, Witherel CE, Yang M, Burdick JA, Wen C, *et al*. Harnessing Tissue-derived Extracellular Vesicles for Osteoarthritis Theranostics. Theranostics. 2022; 12: 207–231.

[16] Buzas EI. The roles of extracellular vesicles in the immune system. Nature Reviews. Immunology. 2023; 23: 236–250.

[17] Zhang L, Zhu XY, Zhao Y, Eirin A, Liu L, Ferguson CM, *et al*. Selective intrarenal delivery of mesenchymal stem cell-derived extracellular vesicles attenuates myocardial injury in experimental metabolic renovascular disease. Basic Research in Cardiology. 2020; 115: 16.

[18] Meng QT, Lu Q, Zhang ZP, Liu JH, Lou Y. Umbilical cord-derived mesenchymal stem cell-derived exosomal MiR-133a-3p protects against myocardial infarction by inhibiting apoptosis. Journal of Biological Regulators and Homeostatic Agents. 2021, 35: 1707–1715.

[19] Schütte JP, Manke MC, Hemmen K, Münzer P, Schörg BF, Ramos GC, *et al*. Platelet-Derived MicroRNAs Regulate Cardiac Remodeling After Myocardial Ischemia. Circulation Research. 2023; 132: e96–e113.

[20] Song R, Dasgupta C, Mulder C, Zhang L. MicroRNA-210 Controls Mitochondrial Metabolism and Protects Heart Function in Myocardial Infarction. Circulation. 2022; 145: 1140–1153.

[21] Sygitowicz G, Sitkiewicz D. Mitochondrial Quality Control: the Role in Cardiac Injury. Frontiers in Bioscience-Landmark. 2022; 27: 96.

[22] Gong Z, Yang J, Dong J, Li H, Wang B, Du K, *et al*. LncRNA HIF1A-AS1 Regulates the Cellular Function of HUVECs by Globally Regulating mRNA and miRNA Expression. Frontiers in Bioscience-Landmark. 2022; 27: 330.

[23] Niu L, Sun N, Kong L, Xu Y, Kang Y. miR-634 inhibits human vascular smooth muscle cell proliferation and migration in hypertension through Wnt4/β-catenin pathway. Frontiers in Bioscience-Landmark. 2021; 26: 395–404.

[24] Fan FY, Deng R, Lai SH, Wen Q, Zeng Y, Gao L, *et al*. Inhibition of microRNA-221-5p induces osteogenic differentiation by directly targeting smad3 in myeloma bone disease mesenchymal stem cells. Oncology Letters. 2019; 18: 6536–6544.

[25] Zhu A, Kang N, He L, Li X, Xu X, Zhang H. MiR-221 and miR-26b Regulate Chemotactic Migration of MSCs Toward HGF Through Activation of Akt and FAK. Journal of Cellular Biochemistry. 2016; 117: 1370–1383.

[26] Zhou Y, Richards AM, Wang P. MicroRNA-221 Is Cardioprotective and Anti-fibrotic in a Rat Model of Myocardial Infarction. Molecular Therapy. Nucleic Acids. 2019; 17: 185–197.

[27] Algoet M, Janssens S, Himmelreich U, Gsell W, Pusovnik M, Van den Eynde J, *et al*. Myocardial ischemia-reperfusion injury and the influence of inflammation. Trends in Cardiovascular Medicine. 2023; 33: 357–366.

[28] Saito Y, Oyama K, Tsujita K, Yasuda S, Kobayashi Y. Treatment strategies of acute myocardial infarction: updates on revascularization, pharmacological therapy, and beyond. Journal of Cardiology. 2023; 81: 168–178.

[29] Lopez A, Reyna DE, Gitego N, Kopp F, Zhou H, Miranda-Roman MA, *et al*. Co-targeting of BAX and BCL-XL proteins broadly overcomes resistance to apoptosis in cancer. Nature Communications. 2022; 13: 1199.

[30] Zheng H, Liang X, Han Q, Shao Z, Zhang Y, Shi L, *et al*. Hemin enhances the cardioprotective effects of mesenchymal stem cell-derived exosomes against infarction via amelioration of cardiomyocyte senescence. Journal of Nanobiotechnology. 2021; 19: 332.

[31] Zhang J, Lu Y, Mao Y, Yu Y, Wu T, Zhao W, *et al*. IFN-γ enhances the efficacy of mesenchymal stromal cell-derived exosomes via miR-21 in myocardial infarction rats. Stem Cell Research & Therapy. 2022; 13: 333.

[32] Akhmerov A, Parimon T. Extracellular Vesicles, Inflammation, and Cardiovascular Disease. Cells. 2022; 11: 2229.

[33] Han C, Yang J, Sun J, Qin G. Extracellular vesicles in cardiovascular disease: Biological functions and therapeutic implications. Pharmacology & Therapeutics. 2022; 233: 108025.

[34] Montecalvo A, Larregina AT, Shufesky WJ, Stolz DB, Sullivan MLG, Karlsson JM, *et al*. Mechanism of transfer of functional microRNAs between mouse dendritic cells via exosomes. Blood. 2012; 119: 756–766.

[35] Hu S, Huang M, Li Z, Jia F, Ghosh Z, Lijkwan MA, *et al*. MicroRNA-210 as a novel therapy for treatment of ischemic heart disease. Circulation. 2010; 122: S124–S131.

[36] Liu J, Jiang M, Deng S, Lu J, Huang H, Zhang Y, *et al*. miR-93-5p-Containing Exosomes Treatment Attenuates Acute Myocardial Infarction-Induced Myocardial Damage. Molecular Therapy. Nucleic Acids. 2018; 11: 103–115.

[37] Luo Q, Guo D, Liu G, Chen G, Hang M, Jin M. Exosomes from MiR-126-Overexpressing Adscs Are Therapeutic in Relieving Acute Myocardial Ischaemic Injury. Cellular Physiology and Biochemistry: International Journal of Experimental Cellular Physiology, Biochemistry, and Pharmacology. 2017; 44: 2105–2116.